Suppressing quantum noise in gravitational wave interferometers using squeezed states

Author: Dina Aaslyng Dall

Supervisors: Anders Søndberg Sørensen and Emil Zeuthen

Hand in date: 09/08-2020

Abstract

Gravitational waves were first detected in 2015. Since then, gravitational wave interferometers have pushed the limits on what is possible when it comes to measuring changes in length. As classical noise sources have been decreased to a level approaching the quantum noise, quantum noise has begun to play an increasingly important role. The aim of this thesis is to investigate theoretically how quantum noise can be reduced to improve the sensitivity of gravitational wave interferometers further by using squeezed light. To achieve this, the noise spectral density is derived for a standard Mach Zehnder interferometer, and an adapted Mach Zehnder interferometer where the intensity of the laser influence the phase change of the light. As a result, the effect of using squeezed light in the otherwise unused port of the interferometer has been found. For a standard Mach Zehnder interferometer, amplitude squeezed light suppress the quantum noise for all frequencies. For the adapted Mach Zehnder interferometer, broadband amplitude squeezed light decreases the quantum noise for low frequencies, while broadband phase squeezed light decreases the quantum noise for high frequencies. Also, by making the rotation in phase space frequency dependent, it was found that an increased sensitivity for all frequencies can be achieved. The implication of this is that weaker gravitational waves than currently possible are detectable, if the results are implemented.

Contents

1 Introduction

For the first time in history, on September 14th 2015, the Laser Interferometer Gravitational-Wave Observatory (LIGO) detected gravitational waves [1]. Not only is it the first evidence of binary black holes and a confirmation of part of Einstein's theory of general relativity, it also proved that interferometry can be used as a completely new tool to gain knowledge about the universe. The importance of this can hardly be overstated. In 2017, the discovery let to the Nobel Prize in physics being awarded to Weiss, Thorne and Barish for "decisive contributions to the LIGO detector and the observation of gravitational waves" [2].

When two heavy celestial bodies orbit each other - such as the in-spiral and merging of the binary black holes detected in 2015 by LIGO - it creates disturbances in the curvature of space time. These disturbances propagate as waves and cause distances to slightly stretch and shorten. Other sources of gravitational waves are the spinning of slightly non-symmetric neutron stars and, possibly, the inflation after big bang. [3] The miniscule changes in distance is what LIGO and other gravitational wave interferometers such as Virgo interferometer and Kamioka Gravitational Wave Detector (KAGRA) measure using the interference property of light [4, 5, 6].

In an interferometer, a light beam is split into two different arms and later combined. A relative change in distance between the two different arms leads to a change in the phase difference between the two light beams and thereby in their interference.

Currently, LIGO is able to detected changes 10^{-4} the width of a proton in distance between its four kilometer long arms [7]. To achieve this incredibly high sensitivity, noise have to be at a minimum. There are several different noise sources, among which are thermal fluctuation of the mirror coating, thermal fluctuations in the suspension system of the mirrors, and seismic activity [4].

Another noise source is quantum noise, or quantum fluctuations, due to Heisenberg's uncertainty principle. There are two sources of quantum noise: shot noise and back action. Shot noise stems from fluctuations in the arrival time of photons at the detectors while back action stems from fluctuations in radiation pressure at the mirrors of the interferometer. At low frequencies, the quantum noise is dominated by back action while at higher frequencies, it is dominated by shot noise. Both sources of quantum noise originate from vacuum entering the interferometer through the unused port [8, 9].

Employing state-of-the-art technology, LIGO have successfully decreased its various classical noise sources to such an extent, that quantum noise now plays a significant role in the measurements, especially at higher frequencies. This makes it worthwhile to attempt to minimize the quantum noise. A way to achieve this is by injecting broadband squeezed states into the interferometer, decreasing either shot noise or back action. During its third observation run (O3), this has been implemented in LIGO, decreasing the shot noise and achieving a better sensitivity for frequencies above 50 Hz. Thereby the expected detection rate was increased up to 50 %. [10, 11]

However, as the shot noise decreases, the back action increases, making the sensitivity for low frequencies worse. By changing the squeezing angle as a function of frequency, a higher sensitivity may be reached for both high and low frequencies.Recently, this has been tested experimentally by McMuller et al. and Zhao et al., but has not yet been implemented at any gravitational wave interferometers [12, 13].

The improving of the sensitivity of gravitational wave interferometers by using squeezed light is the phenomenon explored in this thesis. The aim of this project is to investigate where the quantum noise arises from in a Mach Zehnder interferometer and in an interferometer, where the phase difference arises from the movement of a mirror in a cavity. Furthermore, I will study how squeezed light can be used to decrease the quantum noise for certain frequencies and how frequency-dependent rotation in phase-space of squeezed vacuum can be used to increase the

sensitivity simultaneously in frequency regions dominated by shot noise and regions dominated by back action.

To achieve this, the necessary background theory of light is briefly introduced in Sec. 2 after which a standard Mach Zehnder interferometer is studied in Sec. 3. This gives the necessary background knowledge to study an adapted Mach Zehnder interferometer, which is more similar to the interferometers used in gravitational wave detection, described in Sec. 4.

2 Theory

2.1 States of light

To understand quantum noise in interferometry, it is necessary to have a quantum description of light. The Hamiltonian for light in a cavity is

$$\hat{H} = \hbar\omega \left(\hat{a}^\dagger \hat{a} + \frac{1}{2} \right) , \tag{1}$$

where $\hat{a}$ is the annihilation operator, $\hat{a}^\dagger$ the creation operator, and ω the frequency of the light. Their commutation relation is $[\hat{a}, \hat{a}^\dagger] = 1$. Using $\hat{a}$ and $\hat{a}^\dagger$, the quadrature operators $\hat{X}' = \frac{1}{2}(\hat{a} + \hat{a}^\dagger)$ and $\hat{P}' = \frac{1}{2i}(\hat{a} - \hat{a}^\dagger)$ can be defined. It follows from the commutation relation between $\hat{a}$ and $\hat{a}^\dagger$ that $[\hat{X}', \hat{P}'] = \frac{i}{2}$. $\hat{X}'$ is proportional to the electric field of the light while $\hat{P}'$ is proportional to the magnetic field. As $\hat{X}'$ and $\hat{P}'$ do not commute, they have an uncertainty relation. This can be shown to be

$$\Delta\hat{X}' \, \Delta\hat{P}' \geq \frac{1}{4} \tag{2}$$

from their commutation relation. The uncertainty is defined as $\Delta\hat{X}' = \sqrt{\langle \hat{X}^2 \rangle - \langle \hat{X} \rangle^2}$ and likewise for $\hat{P}'$.

To visualize a state of light, a phase space picture as seen in Fig. 1 can be used. Here, the circle represents the uncertainty, while φ is the phase of the light and α is the centre of the circle. The time-evolution of the states is $\left| \psi(t=0) \, \mathrm{e}^{-i\omega t} \right\rangle$.

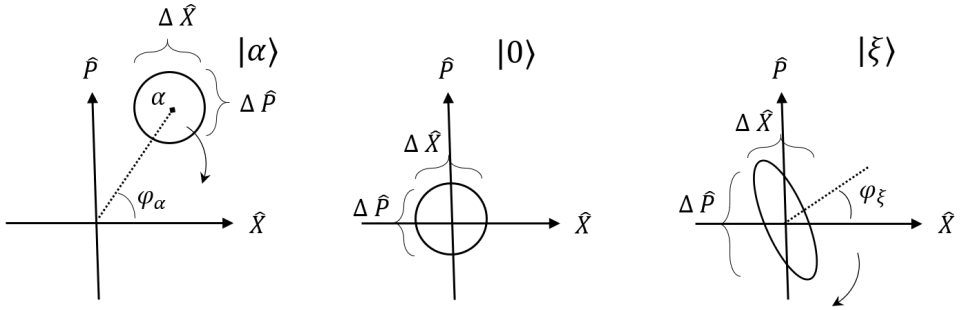

(a) Coherent state (b) Vacuum state (c) Squeezed state

Figure 1: Different states of light shown in phase-space. The circle represents fluctuations in the quadrature operators due to Heisenberg's uncertainty principle with the center of the circle being the average value. Seen in a lab frame, all the states rotate as a function of time, as indicated by the arrow.

A coherent state, $|\alpha\rangle$, which is the light from e.g. a laser, have the property $\hat{a}|\alpha\rangle = \alpha|\alpha\rangle$. Its fluctuations in $\hat{X}$ and $\hat{P}$ is equal and minimum - i.e. $\Delta X = \Delta P = \frac{1}{2}$, this is called the standard quantum limit (SQL). The average number of photons, $\langle \hat{a}^\dagger \hat{a} \rangle$, are $|\alpha|^2$.

Through this report, the $\hat{X}'$-quadrature will also be called the amplitude quadrature, while the $\hat{P}'$-quadrature will be called the phase quadrature. This is because if a coherent state $|\alpha\rangle$ with $\alpha \in \mathbb{R}$ experience a small change of its phase, this will mainly be seen in the $\hat{P}'$-quadrature, while a small change in its amplitude, will be seen in the $\hat{X}'$-quadrature.

In the case, where $\alpha = 0$, it is a vacuum state. Due to the uncertainty relation Eq. 2, there will still be fluctuations of the electric and magnetic field even when no photons are present. These vacuum fluctuation will play an important role when analyzing the noise in gravitational wave interferometers.

To decrease the fluctuations in one quadrature at the expense of larger fluctuations in the other quadrature, one could imagine that the circle representing the uncertainty got "squeezed" into an oval, such that either $\Delta\hat{X}' < 1/2$ or $\Delta\hat{P}' < 1/2$, as seen in Fig. 1c. Such a state is called a squeezed state, $|\xi>$. It is described by the squeezing parameter $\xi = re^{i\varphi_\xi}$, where r is how squeezed the light is, and $\varphi_{sq.}i$ the squeezing angle.

The squeezing operator, $\hat{S}_\xi$, works on a vacuum state such that $\hat{S}_\xi |0\rangle = |\xi\rangle$. In the case of ideally squeezed light, i.e. $\Delta\hat{X}' \, \Delta\hat{P}' = \frac{1}{4}$,

$$\begin{aligned} \hat{S}^\dagger(\xi)\hat{a}(\omega)\hat{S}(\xi) &= \hat{a}(\omega)\cosh(r) - \hat{a}^\dagger(-\omega)\mathrm{e}^{i\theta_{sq.}/2}\sinh(r) \\ \hat{S}^\dagger(\xi)\hat{a}^\dagger\hat{S}(\xi) &= \hat{a}^\dagger\cosh(r) - \hat{a}\mathrm{e}^{-i\theta_{sq.}/2}\sinh(r) \ . \end{aligned} \tag{3}$$

2.2 Continuum case

In Eq. 1, the Hamiltonian was for a cavity, and as such, $\hat{a}$ and $\hat{a}^\dagger$ were operators for discretely quantized light. To describe light in free space, one could imagine that the cavity becomes infinitely large. At this limit, $\hat{a}$ and $\hat{a}^\dagger$ has the commutation relation in the time and frequency domain

$$[\hat{a}(t), \hat{a}^\dagger(t')] = \delta(t - t') \tag{4}$$

$$[\hat{a}(\omega), \hat{a}^\dagger(\omega')] = \delta(\omega - \omega') \ . \tag{5}$$

Combining the Eq. 3 and Eq. 5 it can be shown that for $|\xi\rangle$ or $|0\rangle$

$$\begin{aligned} \left\langle \hat{X}^\dagger(\omega')\hat{X}(\omega) \right\rangle = \left\langle \hat{X}(\omega)\hat{X}^\dagger(\omega') \right\rangle &= \frac{1}{4}S^{-1} \ \delta(\omega - \omega') \\ \left\langle \hat{P}^\dagger(\omega')\hat{P}(\omega) \right\rangle = \left\langle \hat{P}(\omega)\hat{P}^\dagger(\omega') \right\rangle &= \frac{1}{4}S \ \delta(\omega - \omega') \ , \end{aligned} \tag{6}$$

if $\varphi_{sq.} = 0$, where $S = \mathrm{e}^{2r}$ is the amount of squeezing.

2.3 Heisenberg's and Schrödinger's picture

When studying the time evolution of a system, which is necessary when studying a time-dependent gravitational wave, it can be described in different ways.

In the Schrödinger picture, the states are time-dependent while the operators are not. A change due to a gravitational wave would therefore be seen in the state of the light. On the other hand, in the Heisenberg's picture, the time evolution is in the operators while the states are time-independent.

These different ways of looking at the same system are interchangeable. In this report, Heisenberg's picture has been used, as it in this cases proves to be a more simple approach.

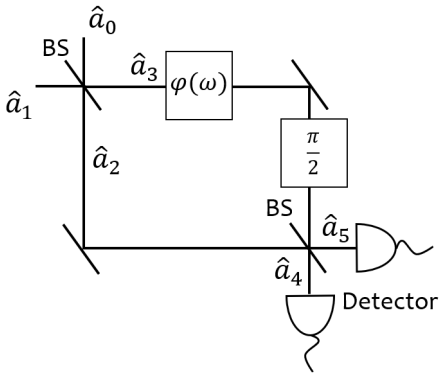

Figure 2: The set up of a Mach Zehnder interferometer. Light, associated with the annihilation operator $\hat{a}$, enters the interferometer through the beam splitter (BS) at the top, left corner and is split into two paths. One path experiences a phase shift, $\varphi(\omega)$, and an additional phase shift of $\pi/2$ after which the two beams are combined in the second beam splitter. Finally, the output is measured at the two detectors.

3 Mach-Zehnder interferometer

To measure gravitational waves, an interferometer is used. An interferometer works by splitting a light beam and later combining the two resulting beams again. A change in the relative optical path length between the two arms will change the interference pattern, which is detected.

To first study a simpler model, I analyse how a Mach-Zehnder interferometer with a phase shift φ works, as seen in Fig. 2. In the interferometer, the light first enters the beam splitter and is split equally into two arms, one of which has a phase shift $\varphi(t)$, which is the signal we want to measure. $\varphi(t)$ is not affected by the laser. Then, the two beams are combined again in a second 50/50 beam splitter. Furthermore, a phase-shift of $\mathrm{e}^{i\pi/2}$ is added to arm 3. This balances the intensity so that the intensity will be equal at the two detectors when $\varphi = 0$. Finally, the intensity at the two detectors are measured and subtracted from each other.

With the numbering of the different beams seen on Fig. 2, the measured difference in intensity is

$$\hat{\mathrm{I}} = \hat{a}_4^\dagger \hat{a}_4 - \hat{a}_5^\dagger \hat{a}_5 \ . \tag{7}$$

Using the input output relation for the beam splitters

$$\begin{aligned} \hat{a}_0^\dagger &\to \frac{1}{\sqrt{2}}(\hat{a}_2^\dagger + i\ \hat{a}_3^\dagger) \\ \hat{a}_1^\dagger &\to \frac{1}{\sqrt{2}}(i\ \hat{a}_2^\dagger + \hat{a}_3^\dagger) \ , \end{aligned} \tag{8}$$

and knowing that the phase takes $\hat{a} \to \hat{a}\mathrm{e}^{i\varphi}$, the input-output relation of the interferometer is

$$\begin{aligned} \hat{a}_4^\dagger &\to -\frac{1}{2}\left((\mathrm{e}^{-i\varphi} + i)\ \hat{a}_0^\dagger + (i\ \mathrm{e}^{-i\varphi} + 1)\ \hat{a}_1^\dagger\right) \\ \hat{a}_5^\dagger &\to \ \ \frac{1}{2}\left((i\ \mathrm{e}^{-i\varphi} + 1)\ \hat{a}_0^\dagger - (\mathrm{e}^{-i\varphi} + i)\ \hat{a}_1^\dagger\right) \ . \end{aligned} \tag{9}$$

This can be used to find the intensity difference between the two detectors as a function of the phase and the incoming light:

$$\hat{\mathrm{I}} = \hat{a}_4^\dagger \hat{a}_4 - \hat{a}_5^\dagger \hat{a}_5 = \sin(\varphi)\ (\hat{a}_1^\dagger \hat{a}_1 - \hat{a}_0^\dagger \hat{a}_0) + \cos(\varphi)\ (\hat{a}_1^\dagger \hat{a}_0 + \hat{a}_0^\dagger \hat{a}_1) \ . \tag{10}$$

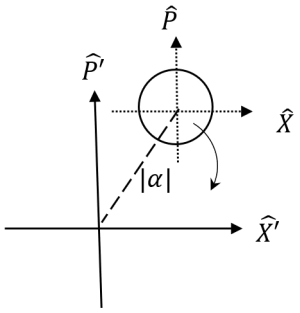

Figure 3: A coherent state seen in two different coordinate frames.

Here, I will do two things. Firstly, I move to a reference frame with origo at the expectiation value of $\hat{a}$ and with fluctuations $\delta\hat{a}$ around this origo, as seen in Fig. 3. Since $\langle\hat{a}\rangle = \alpha(t = 0)\ \mathrm{e}^{-i\omega t}$, this means the origo rotates in space. For coherent and squeezed light, the coordinate transformation is

$$\begin{aligned} \hat{a}_{coh} &= \alpha_{coh}(t=0)\ \mathrm{e}^{-i\omega_L t} + \delta\hat{a}_{coh}\mathrm{e}^{-i\omega_L t} \\ \hat{a}_{sq.} &= \delta\hat{a}_{sq.}(t=0)\ \mathrm{e}^{-i\omega_{sq.} t}\ , \end{aligned} \tag{11}$$

where ω_L is the frequency of the laser (i.e. the coherent light) and $\omega_{sq.}$ the frequency of the squeezed light.

Secondly, I move from a lab frame to a rotating laser frame in which the phase of the laser does not oscillate with time. This is done by defining a new creation operator $\hat{\tilde{a}} = \hat{a}\ \mathrm{e}^{i\omega_L t}$, where ω_L is the frequency of the laser.

Using this and assuming coherent light is sent through the arm 1 while squeezed is sent through arm 0, I find

$$\hat{\mathrm{I}}(\mathrm{t}) = \sin(\varphi)\ \left((\tilde{\alpha}_1^* + \delta\hat{\tilde{a}}_1^\dagger)(\tilde{\alpha}_1 + \delta\hat{\tilde{a}}_1) - \delta\hat{\tilde{a}}_0^\dagger\delta\hat{\tilde{a}}_0\right) + \cos(\varphi)\ \left((\tilde{\alpha}_1^* + \delta\hat{\tilde{a}}_1^\dagger)\delta\hat{\tilde{a}}_0 + \delta\hat{\tilde{a}}_0^\dagger(\tilde{\alpha}_1 + \delta\hat{\tilde{a}}_1)\right)\ . \tag{12}$$

To find the noise spectra, the relevant term is $\left\langle \hat{I}(\omega)^\dagger \hat{I}(\omega) \right\rangle$ [14]. It is therefore necessary first to Fourier transform $\hat{I}(t)$ and thereafter find the expectation value. To simplify the expression, I omit terms from $\hat{I}(t)$ that in the end will give zero when the expectation value $\left\langle \hat{I}(\omega)^\dagger \hat{I}(\omega) \right\rangle$ is calculated (e.g. terms $\propto \delta\hat{a}$ or $\delta\hat{a}_1^\dagger\delta\hat{a}_1$).

Furthermore, I am interested in the limit, where the noise is the same order of magnitude as the signal - if the noise is much smaller than the signal, other sources of noise will dominate instead. When finding $\left\langle \hat{I}(\omega)^\dagger \hat{I}(\omega) \right\rangle$ while assuming φ is small, the signal is $\varphi^2|\alpha|^4$. Terms in $\left\langle \hat{I}(\omega)^\dagger \hat{I}(\omega) \right\rangle$, which are small compared to the signal, are $\propto \varphi\alpha$, $\varphi^2\alpha^2$, α and $\delta\hat{a}_0^\dagger\delta\hat{a}_0$. In the expression for $\hat{I}(t)$, terms that *only* contribute to small terms or gives zero, when $\left\langle \hat{I}(\omega)^\dagger \hat{I}(\omega) \right\rangle$ is found, are omitted. Using this, Eq. 12 can be written as

$$\hat{\mathrm{I}}(\mathrm{t}) \approx \varphi(t)\ |\alpha|^2 + \tilde{\alpha}^*\ \delta\hat{\tilde{a}}_0(t) + \tilde{\alpha}\ \delta\hat{\tilde{a}}_0^\dagger(t)\ . \tag{13}$$

We are interested in the gravitational wave signal and therefore also in the noise spectral

density as a function of frequency. For this reason, Eq. 13 is Fourier transformed:

$$\begin{aligned}\hat{\mathrm{I}}(\omega) = \mathscr{F}\left(\hat{\mathrm{I}}(\mathrm{t})\right) &= \varphi(\omega)|\alpha|^2 + \int_{-\infty}^{\infty} dt \frac{\tilde{\alpha}^*}{\sqrt{2\pi}} \mathrm{e}^{i\omega t} \delta\hat{\tilde{a}}_0 + \int_{-\infty}^{\infty} dt \frac{\tilde{\alpha}}{\sqrt{2\pi}} \mathrm{e}^{i\omega t} \delta\hat{\tilde{a}}_0^\dagger \\ &= \varphi(\omega)|\alpha|^2 + \tilde{\alpha}^*\ \delta\hat{\tilde{a}}_0(\omega) + \tilde{\alpha}\ \delta\hat{\tilde{a}}_0^\dagger(-\omega)\ , \end{aligned} \tag{14}$$

where to Fourier transform convention

$$\hat{a}(\omega) = \int_{-\infty}^{\infty} dt \frac{\hat{a}(t)}{\sqrt{2\pi}} \mathrm{e}^{i\omega t} \tag{15}$$

$$\hat{a}^\dagger(\omega) = \int_{-\infty}^{\infty} dt \frac{\hat{a}(t)^\dagger}{\sqrt{2\pi}} \mathrm{e}^{-i\omega t} \tag{16}$$

is used. This convention means that the signal will lie on the two sidebands ω and $-\omega$ around $\omega = 0$ in the laser frame [14]. I.e., in the lab frame the sidebands are at $\omega_L \pm \omega$.

Without loss of generality, the coherent light can be chosen to be real, since the important quantity is the relative phase difference between the coherent and squeezed light. Letting $\alpha = \alpha^* = |\alpha|$ Eq. 14 can be written in term of the quadrature operator $\hat{X}(\omega) = \frac{1}{2}(\delta\hat{\tilde{a}}(\omega) + \delta\hat{\tilde{a}}^\dagger(-\omega))$

$$\hat{I}(\omega) = \varphi(\omega)|\alpha|^2 + 2|\alpha|\hat{X}(\omega)\ . \tag{17}$$

It is not the magnitude of the quantum noise on its own that is important, but rather its magnitude relative to the magnitude of the signal: the signal to noise-ratio. Therefore, the intensity is normalized with regard to the strength of the signal, i.e., the factor before φ.

$$\hat{I}_{\mathrm{norm}} = I_s + \delta I = \varphi + \frac{2\ \hat{X}_0}{|\alpha|}\ . \tag{18}$$

Here, $\hat{I}_{\mathrm{norm}}$ is the normalized intensity difference, $\hat{I}_s$ is the signal, while $\delta\hat{I}$ is the fluctuations around $\hat{I}_s$.

To understand the quantum noise, I am interested in the symmetrized noise spectral density $\mathcal{S}_{\delta I}$ [15, 14]:

$$\mathcal{S}_{\delta I}\delta(\omega - \omega') = \frac{1}{2}\langle \delta\hat{I}^\dagger \delta\hat{I} + \delta\hat{I}\delta\hat{I}^\dagger \rangle\ . \tag{19}$$

Using Eq. 3, the noise spectral density becomes

$$\mathcal{S}_{\delta I}\delta(\omega - \omega') = \frac{2}{|\alpha|^2}\langle \hat{X}^\dagger\hat{X} + \hat{X}\hat{X}^\dagger \rangle = \frac{S^{-1}}{|\alpha|^2}\delta(\omega - \omega')\ . \tag{20}$$

First, let us consider the δ-function on the right hand side. Vacuum fluctuations at one frequency are independent of vacuum fluctuations at any other frequency. If $\omega \neq \omega'$, the δ-function will therefore be 0. At $\omega - \omega'$, $\delta(\omega - \omega')$ diverges. This happens since it was assumed the measurement would go from $t = -\infty$ to $t = \infty$ when taking the Fourier transform. In an infinite amount of time, there would be an infinite amount of quantum noise. Even though this might seem problematic, it is not, because in a measurement taken over an infinite amount of time, the signal will likewise be infinitely large. In reality, the measurement does of course not run for an infinite amount of time.

To find the noise spectral density, the δ-function on the right hand side is therefore cancelled with the δ-function on the left hand side to get

$$\mathcal{S}_{\delta I} = \frac{S^{-1}}{|\alpha|^2} \tag{21}$$

In the case, where coherent light is sent into the interferometer in one port while vacuum enters in the other, $S^{-1} = 1$ and $\mathcal{S}_{\delta I} = \alpha^{-2}$. This is as expected since the fluctuations on α for a coherent state is $Var(\alpha) = \alpha$. The higher intensity of the beam, the less quantum noise there will be relative to the signal.

If $r > 0$, $S^{-1} < 1$ and the vacuum is squeezed in the amplitude quadrature. This decreases $\mathcal{S}_{\delta I}$ making the signal less noisy. By letting $r \to \infty$, $S^{-1} \to 0$ and there will be no quantum noise on the signal! One might question whether this obeys Heisenberg's uncertainty principle but as $r \to \infty$ the uncertainty on the intensity becomes infinitely large.

Important to note here is that φ did not depend on the intensity of the light. When measuring gravitational waves, the laser intensity exerts a force on a mirror leading to a change of phase, just like the gravitational wave does. Letting $r \to \infty$, which removes the quantum noise on the phase measurement above, would, as mentioned, create in infinitely large uncertainty on the intensity of the light. This leads to an infinitely large uncertainty on the radiation pressure on the mirror.

To see how the quantum noise might be minimized in gravitational wave measurements, let us therefore consider what happens, if the phase difference arises from movement of a mirror in a cavity, as is the case at LIGO. This is done in Sec. 4.

4 Interferometer with a cavity

To improve the model of Sec. 3, a cavity can be added in one arm, where the movement of one mirror leads to the phase change, which causes the interference pattern. This is a model more similar to how LIGO and other gravitational wave observatories work.

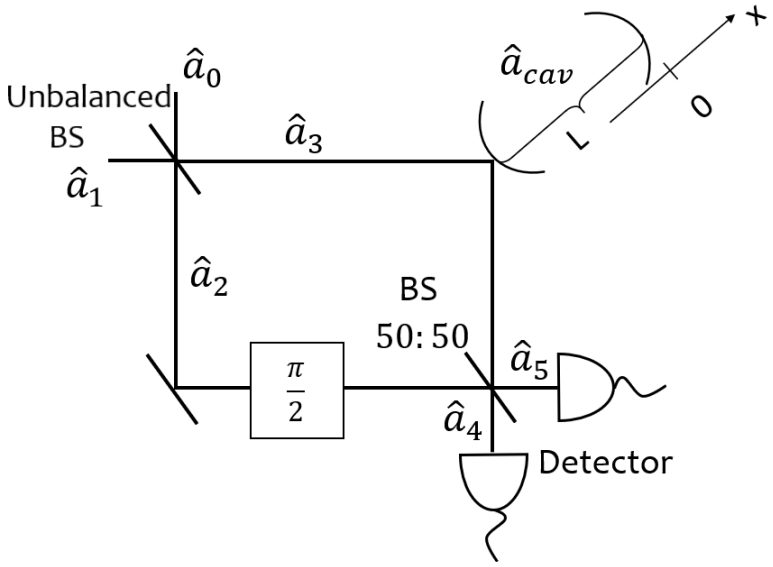

Figure 4

The setup of the interferometer is as seen in Fig 4. It should not be considered a sketch of how an actual gravitational wave interferometers would be constructed. Instead, it is a mathematical consistent model that captures the main aspect of gravitational wave interferometers. It produces displaced squeezed states, that interacts with a cavity whose length can be changed by a gravitational wave, and homodyne detection, which is used to read out the signal from the light beam.

First, light enters the first beam splitter after which it is split into two different paths. Unlike

the example looked at in Sec. 3, the first beam splitter is unbalanced, letting only a fraction of the light towards to cavity (but enough to measure something!) while the rest travels through the other arm.

Using the numbering seen on Fig. 4, a phase shift of $\varphi = \frac{\pi}{2}$ is imposed on the beam in arm 2 - this phase shift selects which quadrature operator from the arm 3 is being studied. In arm 3, the light is being rotated in phase-space such that light originally squeezed along the $\hat{X}$- or $\hat{P}$-quadrature can be oriented in any direction, as seen in Fig 6. This rotation can be frequency dependent. Afterward, the light enters the cavity, whose length can be changed by a gravitational wave.

Finally, the two beams from arm 2 and arm 3 is merged in the second, balanced beam splitter, and the intensity of at the two detectors are substracted from each other. This way acquiring the information carried in the phase of one beam (here beam 3) by combining it with a local oscillator derived from the same laser (here beam 2) is called homodyne detection.

When a gravitational wave pass through Earth, its affect on the interferometer can be modelled as a force acting on the mirror.

4.1 Hamiltonian

To describe the light and find the noise spectral density, it is necessary to describe the motion of the mirror in the cavity, and - using that - to find the input-output relation of the cavity. For both, the Hamilton of the cavity is needed.

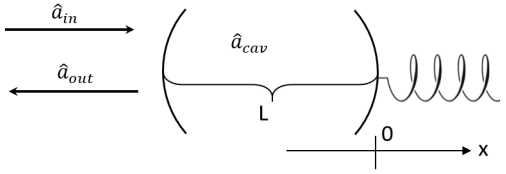

Figure 5: The cavity in the interferometer. The motional degree of freedom for the second mirror is modelled as a harmonic oscillator. A gravitational wave can be seen as a force acting on the mirror, thereby changing the length of the cavity

The Hamilton for the light in the cavity is

$$\hat{H}_{cav} = \hbar\hat{\omega}_{cav}\ \hat{a}^{\dagger}_{cav}\hat{a}_{cav}\ , \tag{22}$$

where ω_{cav} is the frequency of the cavity and depends on the position of the mirror. The vacuum energy $\frac{1}{2}\hbar\omega_{cav}$ has been omitted, as it will not affect the results. In Fig. 5 a sketch of the cavity can be seen.

Writing ω_{cav} in terms of the displacement of the mirror, x, the length of the cavity L and the speed of light c, I have

$$\hat{\omega}_{cav} = \frac{c\pi}{L+\hat{x}} \approx \frac{c\,\pi}{L}\left(1-\frac{\hat{x}}{L}\right) = \omega_0\left(1-\frac{\hat{x}}{L}\right)\ , \tag{23}$$

where it is used that the displacement of the mirror is much smaller than the length of the cavity, $x << L$. ω_0 is the frequency of $\hat{a}_{cav}$ if $x = 0$. Using this, Eq. (22) can be written as

$$\hat{H}_{cav} \approx \hbar\omega_0\hat{a}^{\dagger}_{cav}\hat{a}_{cav}(1-\frac{\hat{x}}{L})\ . \tag{24}$$

4.2 Movement of the mirror

Describing the mirror as a damped, harmonic oscillator, the equations of motion that governs its movement is

$$\dot{\hat{x}}(t) = \frac{\hat{p}(t)}{m} \tag{25}$$

$$\dot{\hat{p}}(t) = -m\ \omega_m^2\ \hat{x}(t) - \gamma\ \hat{p}(t) + \hat{F}_{ba}(t) + \hat{F}_d(t) + \hat{F}_s(t) \tag{26}$$

where $\hat{x}$ is the position-operator of the mirror, $\hat{p}$ the momentum operator of the mirror, ω_m is mirror's mechanical frequency, γ is the damping factor, $\hat{F}_{ba}$ is the back action force, $\hat{F}_d$ is a diffusive force, and $\hat{F}_s$ is the signal (caused by a gravitational wave). Back action is caused by the radiation pressure on the mirror. The diffusive force stems from the dampening of the system.

The back action force can be found using Hamilton's equation

$$F_{ba} = \dot{p}_{cav} = -\frac{\partial H_{cav}}{\partial x} = \frac{\hbar\omega_0}{L}\ \hat{a}_{cav}^\dagger \hat{a}_{cav} \tag{27}$$

$$\approx \frac{\hbar\omega_0}{L}\ (|\alpha_{cav}|^2 + \alpha_{cav}^* \delta\hat{a}_{cav} + \alpha_{cav}\ \delta\hat{a}_{cav}^\dagger) \tag{28}$$

In the last step, the coordinat transformation from Eq. (11) is used and the term $\delta\hat{a}_{cav}^\dagger \delta\hat{a}_{cav}$ is omitted as it is small compared to the terms $\propto \alpha_{cav}$

To solve the system of equations, I let $\hat{x} \to \langle\hat{x}\rangle + \delta\hat{x}$, similar to the coordinat transformation in Eq. (11). $\langle\hat{x}\rangle$ is the average displacement of the mirror due to the average radiation pressure, while $\delta\hat{x}$ is fluctuations around this new equilibrium.

To find $\langle\hat{x}\rangle$, Eq. (26) needs to be solved for the terms which are constant in time. This, however, depends on α_{cav}, which in itself depends on $\hat{x}$, as can be seen in Eq. (39). The consequence is a non-linear set of equations which cannot easily be solved analytically. Instead, a numerical solution is possible. The exact value of $\langle\hat{x}\rangle$ is less important for these calculations.

The time-dependence, and therefore both the noise and the signal, lies in $\delta\hat{x}$. To find an expression for $\delta\hat{x}$, the time-dependent parts of Eq. (25) and 26 is set equal to each other:

$$\dot{\delta\hat{x}} = \frac{\hat{p}}{m} \tag{29}$$

$$\dot{\hat{p}} = -m\ \omega_m^2\ \delta\hat{x} - \gamma\ \hat{p} + \frac{\hbar\omega_0}{L}\ (\alpha_{cav}^* \delta\hat{a}_{cav} + \alpha_{cav}\ \delta\hat{a}_{cav}^\dagger) + \hat{F}_d + \hat{F}_s \tag{30}$$

To solve this, the Fourier transform is found

$$-i\ \omega\ \delta\hat{x}(\omega) = \frac{\hat{p}(\omega)}{m}$$

$$-i\ \omega\ \hat{p}(\omega) = -m\ \omega_m^2\ \delta\hat{x}(\omega) - \gamma\ \hat{p}(\omega) + \frac{\hbar\omega_0}{L}\ \left(\alpha_{cav}^* \delta\hat{a}_{cav}(\omega) + \alpha_{cav}\ \delta\hat{a}_{cav}^\dagger(-\omega)\right) + \hat{F}_d(\omega) + \hat{F}_s(\omega) \tag{31}$$

The solution to which is

$$\delta\hat{x}(\omega) = \chi_m \left(\frac{\hbar\omega_0}{L}\ \left(\alpha_{cav}^* \delta\hat{a}_{cav}(\omega) + \alpha_{cav}\ \delta\hat{a}_{cav}^\dagger(-\omega)\right) + \hat{F}_d(\omega) + \hat{F}_s(\omega) \right) . \tag{32}$$

Here, the susceptibility

$$\chi_m = \frac{1}{m(i\gamma\omega + \omega^2 - \omega_m^2)} \tag{33}$$

is a measure of how easily the mirror is being moved by a force.

4.3 Input-output relation of the cavity

Now, that there is an expression for the movement of the mirror in the cavity, the input-output relation of the cavity can be found. To do this, the equation of motion for the light in the cavity needs to be solved.

The equation of motion for the light in the cavity is [16]

$$\dot{\hat{a}}_{cav} = -\kappa\ \hat{a}_{cav} + \sqrt{2\kappa}\ \hat{a}_{in} + \frac{i}{\hbar}\ [\hat{H}_{cav}, \hat{a}_{cav}] \tag{34}$$

$$\hat{a}_{out} = \hat{a}_{in} - \sqrt{2\kappa}\ \hat{a}_{cav} \tag{35}$$

Here, $1/\kappa$ is the cavity field decay rate, $\hat{a}_{in}$ is the incoming light in the cavity, $\hat{a}_{cav}$ is the light in the cavity, and $\hat{a}_{out}$ is the outgoing light from the cavity, as seen on Fig. 5.

Rewriting Eq. (34) in the laser frame, $\hat{\tilde{a}} = \hat{a}\ \mathrm{e}^{i\omega_L t}$, using the product rule on the left hand side, and cancelling all factors $\mathrm{e}^{-i\omega_L t}$, I get

$$\dot{\hat{\tilde{a}}}_{cav} - i\omega_L \hat{\tilde{a}}_{cav} = -\kappa\hat{\tilde{a}}_{cav} + \sqrt{2\kappa}\hat{\tilde{a}}_{in} + \frac{i}{\hbar}[\hat{H}, \hat{\tilde{a}}_{cav}] \tag{36}$$

Inserting the commutation relation $[\hat{H}, \hat{\tilde{a}}_{cav}] = \hbar\omega_0(\frac{\hat{x}}{L} - 1)\ \hat{\tilde{a}}_{cav}$, which follows from the Hamilton Eq. (24) and the commutation relation $[\hat{a}_{cav}, \hat{a}^\dagger_{cav}] = 1$, and using the coordinate transformation Eq. (11), I find

$$\delta\dot{\hat{\tilde{a}}}_{cav} + \dot{\tilde{\alpha}} - i\omega_L(\delta\hat{\tilde{a}}_{cav} + \tilde{\alpha}_{cav}) = \tag{37}$$

$$-\kappa(\delta\hat{\tilde{a}}_{cav} + \tilde{\alpha}_{cav}) + \sqrt{2\kappa}(\delta\hat{\tilde{a}}_{in} + \tilde{\alpha}_{in}) + i\omega_0(\frac{\langle\hat{x}\rangle - \delta\hat{x}}{L} - 1)\ (\delta\hat{\tilde{a}}_{cav} + \tilde{\alpha}_{cav})$$

$$\tilde{\alpha}_{out} + \delta\hat{\tilde{a}}_{out} = \tilde{\alpha}_{in} + \delta\hat{\tilde{a}}_{in} - \sqrt{2\kappa}\ (\tilde{\alpha}_{cav} + \delta\hat{\tilde{a}}_{cav}) \tag{38}$$

To solve Eq. (37) and Eq. (38), all the small terms are set equal to the small terms, and the large terms are set equal to the large terms.

For the large terms, the new system of equations are

$$\dot{\tilde{\alpha}}_{cav} = \sqrt{2\kappa}\tilde{\alpha}_{in} + \tilde{\alpha}_{cav}(-\kappa - i\omega_0 + i\omega_L + i\frac{\langle\hat{x}\rangle}{L}\omega_0) \tag{39}$$

$$\tilde{\alpha}_{out} = \tilde{\alpha}_{in} - \sqrt{2\kappa}\tilde{\alpha}_{cav} \tag{40}$$

While for the small terms, after Fourier transforming, the system of equations are

$$-i\omega\ \delta\hat{\tilde{a}}_{cav}(\omega) = \sqrt{2\kappa}\ \delta\hat{\tilde{a}}_{in}(\omega) + i\tilde{\alpha}_{cav}\omega_0\frac{\delta\hat{x}(\omega)}{L} + \delta\hat{\tilde{a}}_{cav}(\omega)(i\omega_L - i\omega_0 + i\frac{\langle\hat{x}\rangle}{L}\omega_0 - \kappa) \tag{41}$$

$$\delta\hat{\tilde{a}}_{out}(\omega) = \delta\hat{\tilde{a}}_{in}(\omega) - \sqrt{2\kappa}\delta\hat{\tilde{a}}_{cav}(\omega) \tag{42}$$

As the radiation pressure changes the length of the cavity, the frequency of the cavity's mode, when $\delta\hat{x} = 0$, is changed into $\omega_0' = \omega_0\ (1 - \frac{<\hat{x}>}{L})$. Using ω_0', the detuning, Δ, is defined to be the difference between the laser frequency and that of the cavity $\Delta = \omega_L - \omega_0'$.

From here on, the laser frequency is chosen such that $\Delta = 0$. Furthermore, I chose $\tilde{\alpha} \in \mathbb{R}$, which can be done without loss of generality, by letting the squeezed light be oriented in any direction, since it is the relative phase difference between the coherent and squeezed light that is important.

4.3.1 Input-output relation for α

Eq. (39) and Eq. (40) determine what happens with the intensity of the light as it pass through the cavity. Assuming the laser intensity $\alpha_{in}^{\dagger}\alpha_{in}$ is constant, $\dot{\alpha}_{cav} = 0$, and Eq. (39) and Eq. (40) reads

$$0 = \sqrt{2\kappa}\tilde{\alpha}_{in} - \tilde{\alpha}_{cav}\ \kappa \tag{43}$$

$$\tilde{\alpha}_{out} = \tilde{\alpha}_{in} - \sqrt{2\kappa}\tilde{\alpha}_{cav}\ . \tag{44}$$

Here, it is also used that the laser frequency is chosen such that the detuning is zero, $\Delta = \omega_L - \omega_0' = 0$.

Solving for $\tilde{\alpha}_{cav}$ in Eq. (43) and inserting in Eq. (44), I find

$$\tilde{\alpha}_{out} = \tilde{\alpha}_{in} - \frac{2\kappa}{\kappa}\tilde{\alpha}_{in} = -\tilde{\alpha}_{in} \tag{45}$$

This means the light gets a phase shift of $e^{i\pi}$ but is still real.

To see the phase difference from the movement of the mirror, it is necessary to solve the set of equations Eq. (41) and Eq. (42) containing the small terms.

4.3.2 Input-output relation for $\delta\hat{a}$

To find how the movement of the mirror will change the light, Eq. (41) and Eq. (42) need to be solved. By rewriting Eq. (41) in terms of the quadrature operators $\hat{X} = \frac{1}{2}\ (\delta\hat{\tilde{a}} + \delta\hat{\tilde{a}}^{\dagger})$ and $\hat{P} = \frac{1}{2\,i}\ (\delta\hat{\tilde{a}} + \delta\hat{\tilde{a}}^{\dagger})$, Eq. (41), the complex conjugate of Eq. (41) and Eq. (32) can be written in the form of the matrix equation:

$$\begin{pmatrix} \kappa - i\omega & 0 & i\frac{\omega_0}{2\ L}(\tilde{\alpha}_{cav}^{*} - \tilde{\alpha}_{cav}) \\ 0 & \kappa - i\omega & \frac{\omega_0}{2\ L}(\tilde{\alpha}_{cav}^{*} + \tilde{\alpha}_{cav}) \\ \frac{\hbar\omega_0}{L}(\tilde{\alpha}_{cav}^{*} + \tilde{\alpha}_{cav}) & i\frac{\hbar\omega_0}{L}(\tilde{\alpha}_{cav}^{*} - \tilde{\alpha}_{cav}) & \frac{1}{\chi_m(\omega)} \end{pmatrix} \begin{pmatrix} \hat{X}_{cav} \\ \hat{P}_{cav} \\ \delta\hat{x} \end{pmatrix} = \begin{pmatrix} \sqrt{2\kappa}\ \hat{X}_{in} \\ \sqrt{2\kappa}\ \hat{P}_{in} \\ \hat{F}_s + \hat{F}_d \end{pmatrix} \tag{46}$$

Here, it is still assumed that $\Delta = 0$. It is used that $\delta x(t) = \delta x^{\dagger}(t)$, since it is an observable and must therefore be hermitian, which leads to $\mathscr{F}(\delta x(t)) = \mathscr{F}(\delta x^{\dagger}(t)) = \delta\hat{x}(\omega)$ and $\mathscr{F}(F(t)) = \mathscr{F}(F^{\dagger}(t)) = F(\omega)$.

In Sec. 4.3, the incoming light was chosen to be real and positive. It follows from Eq. (**??**)hat the light in the cavity is also real and positive. Therefore, I let $\alpha_{cav} = \alpha_{cav}^{*} = |\alpha_{cav}|$.

Solving for the inverse of the matrix on the left hand side and using $\tilde{\alpha}_{in} \in \mathbb{R}$, I find:

$$\begin{pmatrix} \hat{X}_{cav} \\ \hat{P}_{cav} \\ \delta\hat{x} \end{pmatrix} = \begin{pmatrix} \frac{1}{\kappa - i\omega} & 0 & 0 \\ \frac{2\chi_m\hbar\omega_0^2|\alpha_{cav}|^2}{(\kappa - i\omega)^2L^2} & \frac{1}{\kappa - i\omega} & -\frac{\chi_m\omega_0|\alpha_{cav}|}{L(\kappa - i\omega)} \\ -\frac{2\chi_m\ \hbar\omega_0|\alpha_{cav}|}{L(\kappa - i\omega)} & 0 & \chi_m(\omega) \end{pmatrix} \begin{pmatrix} \sqrt{2\kappa}\ \hat{X}_{in} \\ \sqrt{2\kappa}\hat{P}_{in} \\ \hat{F}_s + \hat{F}_d \end{pmatrix} \tag{47}$$

Combining Eq. (42) and Eq. (47), the input-output-relation for the quadrature operators are found to be

$$\hat{X}_{out} = \hat{X}_{in}(1 - \frac{2\kappa}{\kappa - i\omega}) = -\hat{X}_{in}\frac{\kappa + i\omega}{\kappa - i\omega} \tag{48}$$

and

$$\begin{aligned}\hat{P}_{out} &= \hat{P}_{in} - \sqrt{2\kappa}\hat{P}_{cav} \\ &= -\hat{P}_{in}\frac{\kappa + i\omega}{\kappa - i\omega} - \hat{X}_{in}\frac{2\cdot 2\kappa\ \hbar\omega_0^2\ |\alpha_{cav}|^2}{(\kappa - i\omega)^2 f(\omega) L^2} + \ \frac{\sqrt{2\kappa}\ \omega_0 |\alpha_{cav}|}{L(\kappa - i\omega) f(\omega)}(\hat{F}_s + \hat{F}_d)\ .\end{aligned} \tag{49}$$

As it can be seen, the cavity gives the outgoing $\hat{X}$-quadrature a frequency-dependent phase compared to the incoming $\hat{X}$-quadrature. However, for the outgoing $\hat{P}$-quadrature, it mixes the incoming $\hat{X}_{in}$- and $\hat{P}_{in}$-quadrature. Importantly, all the information about the signal is also carried by $\hat{P}_{out}$
-quadrature. The interferometer should therefore be tuned to only detect this quadrature.

By defining $\tan(\theta) = \frac{\omega}{\kappa}$, the Lorentzian function $\mathcal{L}(\omega) = \dfrac{\kappa}{\kappa - i\omega} = \dfrac{\kappa}{\sqrt{(\kappa^2 + \omega^2)}}\ \mathrm{e}^{i\theta}$, and using the trigonometric identity $\tan(2\theta) = \frac{2\tan(\theta)}{1-\tan^2(\theta)}$, Eq. (49) can be written as

$$\begin{aligned}\hat{P}_{out} = &- \hat{P}_{in}\mathrm{e}^{i2\theta(\omega)} - \hat{X}_{in}\frac{4\ \hbar\omega_0^2\chi_m(\omega)\ |\alpha_{cav}|^2}{L^2}\mathrm{e}^{i2\theta(\omega)}\frac{|\mathcal{L}(\omega)|^2}{\kappa} \\ &+ \ \frac{2|\mathcal{L}(\omega)|\mathrm{e}^{i\theta(\omega)}\ \omega_0\chi_m(\omega)|\alpha_{cav}|}{\sqrt{2\kappa}L}(\hat{F}_s + \hat{F}_d)\ .\end{aligned} \tag{50}$$

$\mathcal{L}(\omega)$ is a Lorentzian function that describes the respond of the cavity to the gravitational wave frequencies. If the cavity is broad, that is $\frac{\omega}{\kappa} \ll 1$ and $|\mathcal{L}(\omega)| \approx 1$ for the relevant frequencies, the mirror's position is approximately constant in the time it takes for a photon to enter the cavity and exit again. This will be the case for low frequencies but not for high frequencies. For high frequencies, the movement of the mirror in the time it takes the photons to enter and exit the cavity, cannot be assumed constant.

The gravitational force, $\hat{F}_{signal}$ will vary between different interferometers with mirrors of different masses. For this reason, the force is rewritten in terms of the distance, the mirror is moved due to the gravitational wave, $\delta\hat{x}_s$, which is independent of the mass of the mirror:

$$\hat{F}_s = \frac{\delta\hat{x}_s}{\chi_m(\omega)}\ . \tag{51}$$

Defining the constant g, which depends on the interferometer,

$$g = \frac{2\ \omega_0\ |\alpha_{cav}|\sqrt{\hbar}}{L\sqrt{\kappa\ m}}\ , \tag{52}$$

Eq. (50), can be written as

$$\hat{P}_{out} = - \hat{P}_{in}\mathrm{e}^{i2\theta} - \hat{X}_{in}\frac{g^2\ |\mathcal{L}(\omega)|^2}{(i\gamma\omega + \omega^2 - \omega_m^2)}\mathrm{e}^{i2\theta} \tag{53}$$

$$+ \ \frac{\mathrm{e}^{i\theta}\ g\ |\mathcal{L}(\omega)|}{\sqrt{2\hbar m}\ (i\gamma + \omega^2 - \omega_m^2)}\hat{F}_d + \frac{\mathrm{e}^{i\theta}\ g\ |\mathcal{L}(\omega)|\sqrt{m}}{\sqrt{2\hbar}}\delta\hat{x}_s\ . \tag{54}$$

Now, that the input-output relation for the cavity is known, this can be used to analyze the entire interferometer.

4.4 Noise spectral density

By using the input-output of the cavity, it is possible to examine the intensity difference, $\hat{I}$, between the two detectors and find the noise spectral density. The setup of the interferometer can be seen in Fig. 4 and its description in the beginning of Sec. 4.

Using the input-output relation Eq. (8) the intensity difference, $\hat{I}$, between the two detectors is

$$\hat{I} = \hat{a}_4^\dagger \hat{a}_4 - \hat{a}_5^\dagger \hat{a}_5 \xrightarrow{BS} -i\hat{a}_2^\dagger \hat{a}_{3,out} + i\hat{a}_{3,out}^\dagger \hat{a}_2 \ . \tag{55}$$

To select the quadrature operator carrying the information about the signal, $\hat{P}_{out}$, a phase difference of $\mathrm{e}^{i\pi/2}$ is applied to $\hat{a}_2$

$$i\hat{a}_2^\dagger \hat{a}_{3,out} + i\hat{a}_{3,out}^\dagger \hat{a}_2 \xrightarrow{phase} -\hat{a}_2^\dagger \hat{a}_{3,out} - \hat{a}_{3,out}^\dagger \hat{a}_2 \tag{56}$$

$$= -(\alpha_2^* + \delta\hat{a}_2^\dagger)(\alpha_{3,out} + \delta\hat{a}_{3,out}) - (\alpha_{3,out}^* + \delta\hat{a}_{3,out}^\dagger)(\alpha_2 + \delta\hat{a}_2^\dagger) \ , \tag{57}$$

where in the last step, the coordinat transformation Eq. (11) was used.

From 45 I know that $\tilde{\alpha}_{3,out} = -\tilde{\alpha}_{3,in}$. Since the incoming light in the cavity is real, $\tilde{\alpha}_{3,in} = \tilde{\alpha}_{3,in}^*$ and $\tilde{\alpha}_{2,in} = -\tilde{\alpha}_{2,in}^*$. Using this and omitting terms $\propto \delta\hat{a}^\dagger \delta\hat{a}$, as they are small compared to the terms $\propto \alpha$, I find

$$\hat{I} = \tilde{\alpha}_{3,in}(\delta\hat{\tilde{a}}_2 + \delta\hat{\tilde{a}}_2^\dagger) + \tilde{\alpha}_2(\delta\hat{\tilde{a}}_{3,out} - \delta\hat{\tilde{a}}_{3,out}^\dagger) \tag{58}$$

As the first beam splitter is very unbalanced, $\tilde{\alpha}_3 \ll \tilde{\alpha}_2$, this reduces to

$$\hat{I} \approx \tilde{\alpha}_2 \ 2i \ \hat{P}_{3,out} \tag{59}$$

$$= -\hat{P}_{in}\mathrm{e}^{i2\theta} - \hat{X}_{in}\frac{g^2 \ |\mathcal{L}(\omega)|^2}{(i\gamma\omega + \omega^2 - \omega_m^2)}\mathrm{e}^{i2\theta} \tag{60}$$

$$+ \ \frac{\mathrm{e}^{i\theta} \ g \ |\mathcal{L}(\omega)|}{\sqrt{2\hbar m} \ (i\gamma + \omega^2 - \omega_m^2)}\hat{F}_d + \frac{\mathrm{e}^{i\theta} \ g \ |\mathcal{L}(\omega)|\sqrt{m}}{\sqrt{2\hbar}}\delta\hat{x}_s \ . \tag{61}$$

The incoming light of the cavity may be oriented in any direction. This is achieved by squeezing the light sent into the interferometer along the quadrature axis and then rotating it $\varphi(\omega)$ in phase-space before it enters the cavity. The light squeezed along the quadrature axis is described using $\hat{\tilde{X}}$ and $\hat{\tilde{P}}$ while the rotated light is described with $\hat{X}_{in}$ and $\hat{P}_{in}$, as seen in Fig. 6. Note here that both $\hat{X}$ and $\hat{\tilde{X}}$ is in the laser frame, as was defined in Sec. 3.

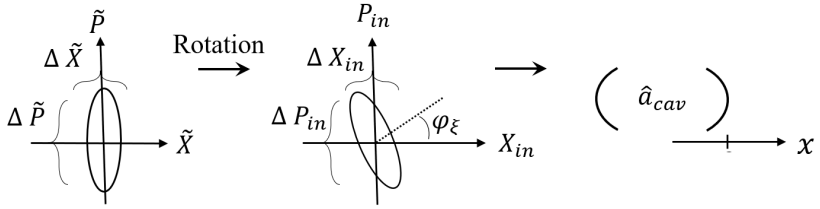

Figure 6: Rotation of squeezed light. First, before the light reaches the cavity

Using the inverse rotation matrix, the relation between $(\hat{\tilde{X}}, \ \hat{\tilde{P}})$ and $(\hat{X}_{in}, \ \hat{P}_{in})$ is

$$\begin{pmatrix} \hat{X}_{in} \\ \hat{P}_{in} \end{pmatrix} = \begin{pmatrix} \cos(\varphi) & \sin(\varphi) \\ -\sin(\varphi) & \cos(\varphi) \end{pmatrix} \cdot \begin{pmatrix} \hat{\tilde{X}} \\ \hat{\tilde{P}} \end{pmatrix} \tag{62}$$

As a function of $\hat{\tilde{X}}$ and $\hat{\tilde{P}}$ the intensity difference of the light then becomes

$$\hat{I} = \alpha_2 \ 2i \ \left(-(-\sin(\varphi)\hat{\tilde{X}} + \cos(\varphi)\hat{\tilde{P}})\mathrm{e}^{i2\theta} - (\cos(\varphi)\hat{\tilde{X}} + \sin(\varphi)\hat{\tilde{P}})\frac{g^2 \ |\mathcal{L}(\omega)|^2}{(i\gamma\omega + \omega^2 - \omega_m^2)}\mathrm{e}^{i2\theta} \right. \tag{63}$$

$$\left. + \ \frac{\mathrm{e}^{i\theta} \ g \ |\mathcal{L}(\omega)|}{\sqrt{2\hbar m} \ (i\gamma + \omega^2 - \omega_m^2)}\hat{F}_d + \frac{\mathrm{e}^{i\theta} \ g \ |\mathcal{L}(\omega)|\sqrt{m}}{\sqrt{2\hbar}}\delta\hat{x}_s \right) \tag{64}$$

As in Eq. (18), the intensity is normalized to the signal to find the signal-to-noise ratio, i.e. divided with the term in front of $\delta\hat{x}_s$:

$$\hat{I}_{\rm norm} = \Bigg(\left(\sin(\varphi)\hat{\tilde{X}} - \cos(\varphi)\hat{\tilde{P}}\right) \mathrm{e}^{i\theta} \frac{\sqrt{2\hbar}}{g\ |\mathcal{L}(\omega)|\sqrt{m}} - (\cos(\varphi)\hat{\tilde{X}} + \sin(\varphi)\hat{\tilde{P}}) \frac{g\ \sqrt{2\hbar}\ |\mathcal{L}(\omega)|\mathrm{e}^{i\theta}}{\sqrt{m}(i\gamma\omega + \omega^2 - \omega_m^2)} \tag{65}$$

$$+\ \ \delta\hat{x}_s + \frac{\hat{F}_d}{m(i\gamma\omega + \omega^2 - \omega_m^2)} \Bigg)\ . \tag{66}$$

This can be written as $\hat{I}_{\rm norm} = \delta\hat{x}_s + \delta I$ as in Eq. (18). To analyse the quantum noise, I am interested in the symmetrized noise spectral density, defined in Eq. (19).

$$\begin{aligned}
\mathcal{S}_{\delta I}\delta(\omega-\omega') =& \frac{1}{2}\langle \delta\hat{I}^\dagger\delta\hat{I} + \delta\hat{I}\delta\hat{I}^\dagger\rangle & (67)\\
=& \frac{1}{2}\langle \Bigg(\left(\sin^2(\varphi)(\hat{\tilde{X}}^\dagger\hat{\tilde{X}} + \hat{\tilde{X}}\hat{\tilde{X}}^\dagger) + \cos^2(\varphi)(\hat{\tilde{P}}^\dagger\hat{\tilde{P}} + \hat{\tilde{P}}\hat{\tilde{P}}^\dagger)\right) \frac{2\hbar}{mg^2\ |\mathcal{L}(\omega)|^2} \\
&+ \left(\cos^2(\varphi)(\hat{\tilde{X}}^\dagger\hat{\tilde{X}} + \hat{\tilde{X}}\hat{\tilde{X}}^\dagger) + \sin^2(\varphi)(\hat{\tilde{P}}^\dagger\hat{\tilde{P}} + \hat{\tilde{P}}\hat{\tilde{P}}^\dagger)\right) \frac{g^2\ 2\hbar\ |\mathcal{L}(\omega)|^2}{m|i\gamma\omega + \omega^2 - \omega_m^2|^2} \\
&- \frac{8\hbar}{m}\frac{(\omega^2-\omega_m^2)}{|i\gamma\omega + \omega^2 - \omega_m^2|^2}\cos(\varphi)\sin(\varphi)\left(\hat{\tilde{P}}^\dagger\hat{\tilde{P}} + \hat{\tilde{P}}\hat{\tilde{P}}^\dagger - (\hat{\tilde{X}}^\dagger\hat{\tilde{X}} + \hat{\tilde{X}}\hat{\tilde{X}}^\dagger)\right) + & (68)\\
&(\hat{F}_d^\dagger\hat{F}_d + \hat{F}_d\hat{F}_d^\dagger)\frac{1}{m^2|i\gamma\omega + \omega^2 - \omega_m^2|^2}\Bigg)\rangle & (69)
\end{aligned}$$

Here, the cross terms have been omitted, since their expectation value is 0. This is due to $\langle\hat{\tilde{X}}^\dagger\hat{\tilde{P}} + \hat{\tilde{P}}^\dagger\hat{\tilde{X}}\rangle = 0$ and $\langle\hat{\tilde{X}}^\dagger\hat{\tilde{P}}\rangle = \langle\hat{\tilde{X}}\hat{\tilde{P}}^\dagger\rangle = -\langle\hat{\tilde{P}}^\dagger\hat{\tilde{X}}\rangle = -\langle\hat{\tilde{P}}\hat{\tilde{X}}^\dagger\rangle$, which follows from Eq. (3) letting $\varphi_{sq.} = 0$.

As in Sec 3 the δ-function are due to the fact that it is assumed the measurement run over an infinite amount of time, and there will therefore be an infinite amount of noise - but likewise, the signal will also become infinitely large.

The diffusive force F_d has the expectation values [17]

$$< \hat{F}_d^\dagger(\omega)\hat{F}_d(\omega') > = 2m\gamma\hbar\omega n(\omega)\delta(\omega-\omega') \tag{70}$$

$$< \hat{F}_d(\omega)\hat{F}_d^\dagger(\omega') > = 2m\gamma\hbar\omega(n(\omega)+1)\delta(\omega-\omega') \tag{71}$$

where $n(\omega) = \left(\mathrm{e}^{\hbar\omega/k_bT_m} - 1\right)^{-1}$ and k_b is Boltzmann's constant, and T_m the temperature of the mirror. In the high temperature limit $k_bT_m \gg \hbar\omega$, this becomes

$$< \hat{F}^\dagger(\omega)\hat{F}(\omega') > + < \hat{F}(\omega)\hat{F}^\dagger(\omega') > \approx 4m\gamma k_bT_m\delta(\omega-\omega') \tag{72}$$

Using Eq. (72) and the expectation value of the quadrature operators from Eq. (6), the noise spectral density Eq. (69) can be written

$$\begin{aligned}
\mathcal{S}_{\delta I} =& \frac{1}{2}\Bigg(\left(\sin^2(\varphi)S^{-1} + \cos^2(\varphi)S\right)\frac{2\hbar}{mg^2\ |\mathcal{L}(\omega)|^2} \\
&+ \left(\cos^2(\varphi)S^{-1} + \sin^2(\varphi)S\right)\frac{g^2\ 2\hbar\ |\mathcal{L}(\omega)|^2}{m|i\gamma\omega + \omega^2 - \omega_m^2|^2} \\
&- \frac{8\hbar}{m}\frac{(\omega^2-\omega_m^2)}{|i\gamma\omega + \omega^2 - \omega_m^2|^2}\left(S - S^{-1}\right) + \frac{4\gamma k_bT_m}{m|i\gamma\omega + \omega^2 - \omega_m^2|^2}\Bigg)
\end{aligned} \tag{73}$$

The dampening of the mirror is contributing both to the shot noise and to the noise from the diffusive force in the last term. To minimize the last term as much as possible, γ is engineered to be extremely small. Therefore, $|i\gamma\omega + \omega^2 - \omega_m^2|^2 \approx |\omega^2 - \omega_m^2|^2$, since the dampening is $\propto \gamma^2$ while the other two terms are $\propto \omega^2$ or $\propto \omega^4$ and, as such, much larger.

When looking at the position sensitivity, the noise from the diffusive force is stronger for low frequencies than high frequencies, which is a property of the noise from seismic activity and thermal fluctuations of the mirror as well [4]. As the aim of this project is to minimize the quantum noise, and this term contribute to the classical noise, it will be omitted from here on.

A characteristic noise spectral density, found by considering which constants $\mathcal{S}_{\delta I}$ depend, is $\mathcal{S}_{char} = \frac{\hbar}{m\ g_{Ligo}^2}$, where $g_{Ligo} = 60 \cdot 2\pi s^{-1}$ is the value of g used in LIGO [18].

Using this, the unitless quantity $\Sigma = \frac{\mathcal{S}_{\delta I}}{\mathcal{S}_{char}}$ is defined. Applying the approximations above, Σ is

$$\Sigma = \Bigg(\left(\sin^2(\varphi)S^{-1} + \cos^2(\varphi)S\right) \frac{g_{Ligo}^2}{g^2|\mathcal{L}(\omega)|^2} + \left(\cos^2(\varphi)S^{-1} + \sin^2(\varphi)S\right) \frac{g^2 g_{Ligo}^2}{|\omega^2 - \omega_m^2|^2} |\mathcal{L}(\omega)|^2 - 4g_{Ligo}^2(\omega^2 - \omega_m^2)\cos(\varphi)\sin(\varphi)\left(S - S^{-1}\right) \Bigg) \ . \tag{74}$$

Here, the first term $\propto g^{-2}$ is the shot noise caused by fluctuations in the arrival time of the photons at the detectors [9]. Increasing the intensity of the laser and thereby g, which is $\propto |\alpha_{cav}|$, would decrease this noise. For high frequencies, this noise dominates. In the setup used in the report g has to be small due to the first beam splitter being unbalanced - real gravitational wave interferometers instead use Michelson interferometers which do not have this problem.

The second term $\propto g^2$ is the backaction. If the intensity of the laser is increased, the uncertainty of the radiation pressure on the mirror is, too, and this noise term becomes larger. For low frequencies, the back action dominates.

The ideal g, that minimizes the quantum noise will therefore be a balancing of the shot noise and quantum noise and depends on which frequency is studied. In reality, g is limited by the possible laser power and shot noise is the dominating quantum noise above 50 Hz in LIGO [10].

In Fig 7 the sensitivity Σ defined in Eq. (74) as a function of frequency of the gravitational wave can be seen for different values of g. There is no squeezing, so $S = 1$. ω_m is set to zero. $\mathcal{L}(\omega)$ depends on κ, that has been set to $\kappa = 450\ Hz$, which is the value LIGO uses [11]. As it can be seen, a low value of g leads to less quantum noise at low frequencies, where the back action dominates, and more quantum noise at higher frequency, where shot noise dominates, while it is opposite for a high value of g. However, at low frequencies other noise sources such as seismic noise, thermal fluctuations and even wind on the building will contribute and the actual sensitivity will therefore be worse than Figure 7 suggest [4]. The (relatively small) gain of sensitivity at low frequencies by choosing a low value of g instead of a higher value will therefore not be worth it, when all noise sources are considered, compared to the (relatively high) lost sensitivity at high frequencies. A high value of g is therefore wanted. However, g is limited by the possible laser intensity.

In the frequency range dominated by shot noise, the sensitivity becomes worse the higher the frequency is. This is not due to the quantum noise but instead arises from $\mathcal{L}(\omega) < 1$, meaning that the frequency is not coupling as well to the interferometer.

In Fig. 8 the sensitivity Σ for different choices of ω_m can be seen. Again, $\kappa = \kappa_{Ligo} = 450\ Hz$ and g is $g = g_{Ligo}$. A high value of ω_m leads to more quantum noise at low frequencies and slightly less at higher frequencies. In reality, such a high ω_m as the blue or even the orange lines in Fig 8 cannot be achieved. To achieve the extremely low γ - which is necessary for the thermal suspension noise not to be dominating, the suspension system is designed such that the

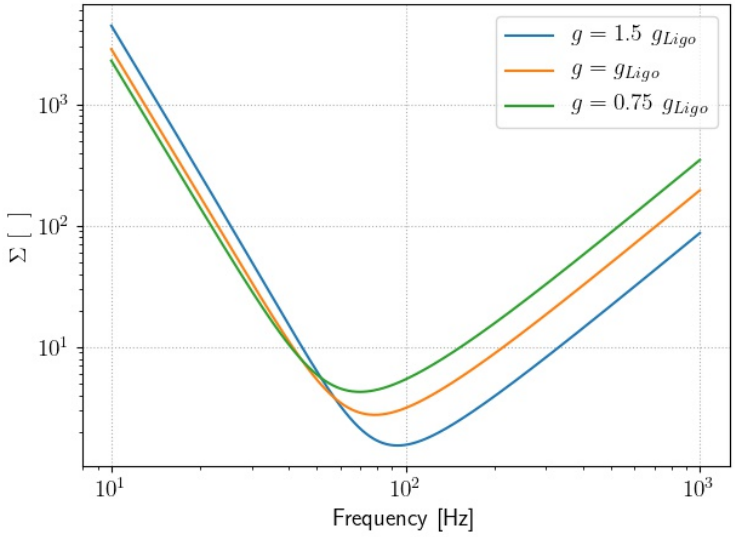

Figure 7: The position sensitivity of the interferometer seen for different values of g. The higher value of g, the better sensitivity for high frequencies. A lower value of g creates a slightly better sensitivity for low frequencies. Only quantum noise is considered. $S = 1,\ \kappa = 450\ Hz,\ \omega_m = 0$.

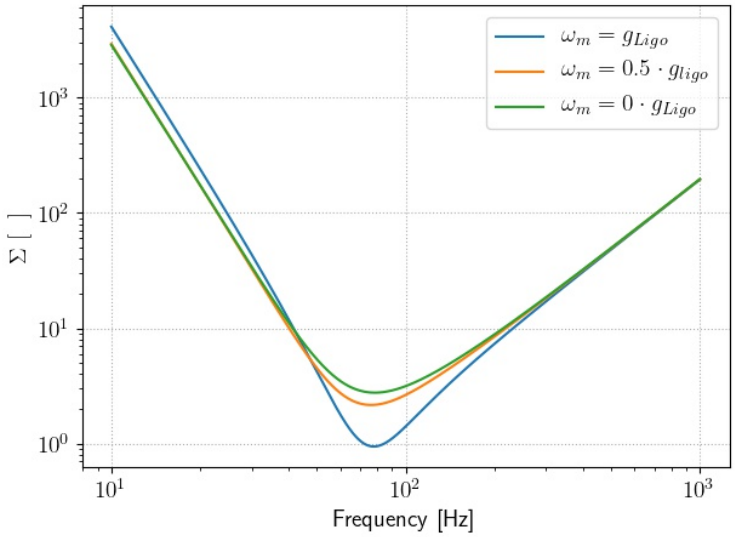

Figure 8: The position sensitivity of the interferometer seen for different values of ω_m. A high value of ω_m creates a better sensitivity for high frequencies. However, experimentally this is infeasible as the dampening needs to be extremely low. Only quantum noise is considered. $S = 1,\ \kappa = 450\ Hz,\ g = 60\ Hz$.

mirror is approaching a free mass [4]. ω_m will therefore by very small, leading to a sensitivity close to the green color line. From here on, it will therefore be assumed that $\omega_m \approx 0$.

To increase the sensitivity, broadband squeezed light can be used - i.e., squeezed light that has the same phase in phase-space for all frequencies. Amplitude squeezed light ($S > 1,\ \varphi = 0$) will decrease the back action while increasing the shot noise, while phase squeezed light ($S > 1,\ \varphi = \frac{\pi}{2}$) will contrarily decrease the shot noise while increasing the back action, as can be

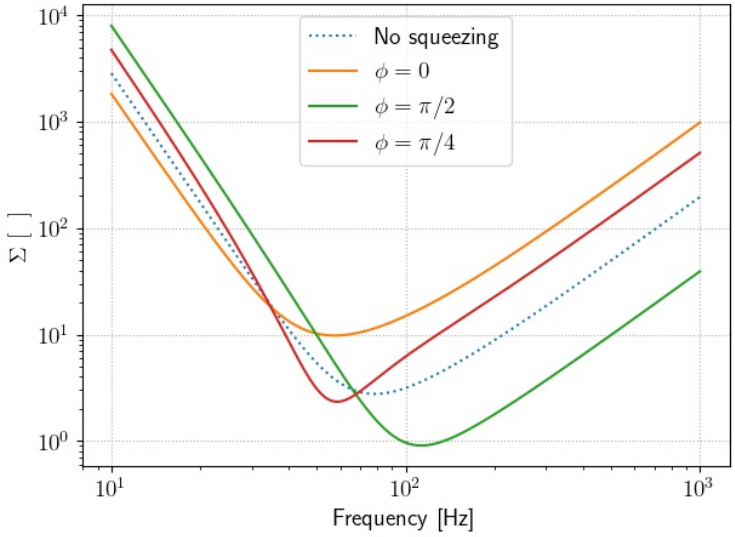

Figure 9: The position sensitivity of the interferometer with broandband squeezed light seen for different values of $\varphi_{sq.}$. $\varphi = 0$ suppress back action while $\varphi = \frac{\pi}{2}$ suppress shot noise. Only quantum noise is considered. $S = 5,\ \kappa = 450\ Hz,\ g = 60\ Hz$.

seen from Eq. (74). This can be seen in Fig. 9 together with the sensitivity without squeezing. Here, $\kappa = \kappa_{Ligo},\ \omega_m = 0,$ and $S = 5$.

From the plot, it is possible to see where back action and shot noise dominates by considering the point where the orange and green line crosses. As was also the case for value of g, the sensitivity gained at higher frequencies by choosing phase squeezed light is much larger than the sensitivity lost at low frequencies. Adding to this that other noise sources such as seismic noise and thermal fluctuations are largest for low frequencies, phase squeezed light is the best choice to increase the sensitivity if broadband squeezed light in used. Effectively, phase squeezed light mimics a higher laser intensity, letting $g \to \sqrt{S}\, g$. As a higher value of g than is currently experimentally feasible is desirable, using broadband squeezing is a way to overcome this. In its third observatory run, LIGO has used broadband squeezed light rotated to suppress a mix of shot noise and back action, optimized to measure the gravitational waves from binary neutron star mergers [10, 11]. This increased the sensitivity above 50 Hz, while decreasing the sensitivity for lower frequencies and lead to a 40 % increase in expected observations in one of its two interferometers and a 50 % increase in its other interferometer. [10]

As can be seen on Fig. 9, for small values of ω the lowest sensitivity is found using $\varphi = 0$ while for high frequencies, the best sensitivity is found using $\varphi = \frac{\pi}{2}$. If the squeezed light, instead of having the same phase for all frequencies, had a frequency-depending phase, it should therefore be possible to select the best sensitivity both at high and low frequencies. Then, it would not be necessary to decide which astrophysical events the interferometer should be tuned to and instead the optimal sensitivity would be achieved for all events. This will especially be important as classical noise at low frequencies is reduced even further and an increase in back action will be more noticeable [13].

To find how the optimal angle depends on frequency Eq. (74) is differentiated with regard to the phase:

$$\frac{\Sigma}{\mathrm{d}\varphi} = -(S - S^{-1})\left(\left(|\mathcal{L}(\omega)|^2 \frac{g^2}{g_{Ligo}^2} - \frac{|\omega^2 - \omega_m^2|^2}{g^2 g_{Ligo}^2 |\mathcal{L}(\omega)|^2}\right)\ \sin(2\varphi) + 2\frac{\omega^2 - \omega_m^2}{g_{Ligo}^2}\cos(2\varphi)\right) = 0\ , \tag{75}$$

which can be rewritten as

$$\tan(2\varphi) = \frac{-2(\omega^2 - \omega_m^2)|\mathcal{L}(\omega)|^2 g^2}{|\omega^2 - \omega_m^2|^2 - g^4|\mathcal{L}(\omega)|^4} \tag{76}$$

For $\omega_m << \omega$, using the tan-identity $\tan(2\theta) = \frac{2\tan(\theta)}{1-\tan^2(\theta)}$, this can be reduced to

$$\varphi = \arctan\left(-\frac{|\mathcal{L}(\omega)|^2 g^2}{\omega^2 - \omega_m^2}\right) + \frac{\pi}{2} \tag{77}$$

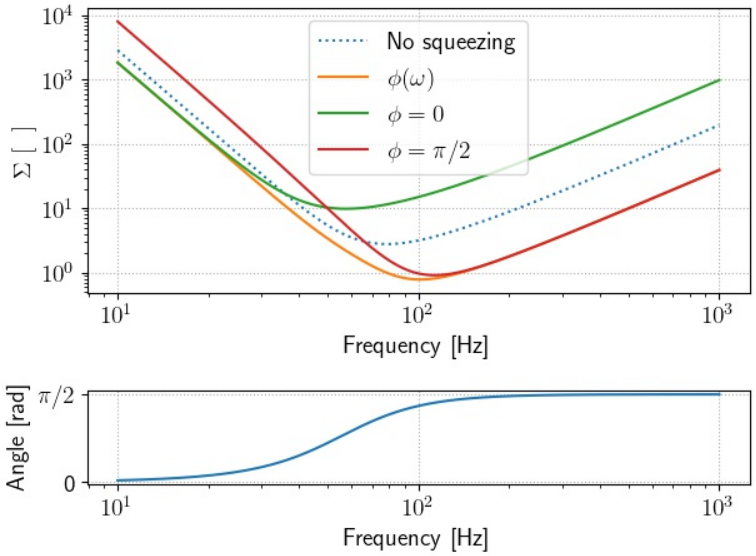

Figure 10: The position sensitivity of the interferometer with frequency dependent squeezed light is seen in orange, while broadband squeezed light is seen in green and red. The dotted line is the sensitivity with vacuum fluctuations. Below, the angle for the frequency-dependent squeezed light is seen. Only quantum noise is considered. $S = 5,\ \kappa = 450\ Hz,\ g = 60\ Hz$.

In Fig 10, the sensitivty with frequency-dependent squeezing can be seen together with sensitivity using broadband squeezing and the sensitivity without squeezing. Furthermore, the optimal angle as a function of frequency can be seen. As can be seen, the frequency-dependent squeezing achieves a better sensitivity than with no squeezing for all frequencies! At low frequencies, the sensitivity matches that of broadband, amplitude squeezed light, while at higher frequencies matching the sensitivity of broadband, phase squeezed light. At frequencies at around $50 \approx Hz$, it outperforms both. If implemented at gravitational wave interferometers, it will thereby be possible to achieve better sensitivity than without squeezing for all frequencies, and better sensitivity for low frequencies than using shot-noise suppressing broadband squeezed light, as LIGO currently do. This means that it will be possible to observe astrophysical events emitting gravitational waves weaker than is currently possible to measure.

To date, this has not been implemented at any gravitational wave interferometers but is planned in both LIGO, Virgo interferometer and KAGRA [13, 12]. However, this technology has been experimentally tested by McCuller et al. and Zhao et al. Independently of each other, they published two papers/articles in April about how the frequency depending rotating of the squeezed light practically could be achieved. Both succeeded with results showing an reduced quantum noise compared to vacuum entering the unused port.

5 Conclusion

In this thesis, the noise spectral density in a standard Mach-Zehnder interferometer with a phase in one arm, that may depend on frequency, but not on the laser power, has been derived. Furthermore, the noise spectral density for an adapted Mach Zehnder interferometer, has been derived. In the adapted Mach-Zehnder interferometer two things have been changed. One, the phase stems from a cavity with one movable mirror and, two, the first beam splitter is very unbalanced, letting only a fraction of the light to the cavity. In both cases, a strong coherent beam enters one port of the interferometer while either vacuum or squeezed vacuum enters the other port.

Fundamentally, the quantum noise is a consequence of Heisenberg's uncertainty relation and stems from the two quadrature operators of light not commuting.

In both interferometers, has been found that the quantum noise arises from vacuum entering the unused port. For the standard Mach Zehnder interferometer, inserting amplitude squeezed vacuum in the otherwise unused port decreases the signal-to-noise ratio. In theory, if infinitely squeezed light could be produced, the quantum noise would go to zero. Similar results can be gained by increasing the intensity of the laser.

The adapted Mach-Zehnder interferometer with a cavity closer resembles the interferometers used by LIGO and other gravitational wave observatories, as the phase stems from the movement of a mirror in a cavity. Here, there are two different quantum noise sources both stemming from Heisenberg's uncertainty principle. One, shot noise, dominates the quantum noise spectrum for high frequencies, and stems from fluctuations in arrival time of the photons at the detectors. The other, back action, dominates the quantum noise spectrum at low frequencies, and stems from fluctuations in radiation pressure on the mirror. Classical noise sources such as seismic activity also plays a vital role at especially lower frequencies.

By inserting broadband squeezed light into the otherwise unused port of the interferometer, a higher laser power can be mimicked. For amplitude squeezed light, back action is decreased but at the expense of more shot noise. As such, the sensitivity for low frequencies is improved while the sensitivity for high frequencies is worsened. For phase squeezed light, shot noise is decreased at the expense of more back action. This worsen the sensitivity for low frequencies while the sensitivity for high frequencies is improved. This has already been implemented at LIGO, where using broadband squeezed light to effectively increase the intensity in the cavity led to an increased amount of observations.

The fact that squeezing in different quadratures is better for different frequencies indicates that an overall improvement in sensitivity can be achieved if the squeezed light is rotated in phase space as a function of frequency. The optimal angle for the squeezed light has been derived, which produces amplitude squeezed light at low frequencies and phase squeezed light at high frequencies. Using this angle produces better sensitivity than vacuum for all frequencies and outperforms both amplitude and phase squeezed light at around 50 Hz for the interferometer studied. As such, implementing it at gravitational wave observatories will increase the overall amount of observations and make observations possible from events that, at the moment, produce too weak a signal to measure. This has not been attained yet, as it is experimentally challenging, but is planned to implemented at LIGO, Virgo interferometer and KAGRA.

References

[1] Benjamin P Abbott, Richard Abbott, TD Abbott, MR Abernathy, F Acernese, K Ackley, C Adams, T Adams, P Addesso, RX Adhikari, et al. Properties of the binary black hole merger gw150914. *Physical review letters*, 116(24):241102, 2016.

[2] The Royal Swedish Academy of Sciences. Press release: The nobel prize in physics 2017. 2017.

[3] James B Hartle. *Gravity: An introduction to Einstein's general relativity*. American Association of Physics Teachers, 2003.

[4] Junaid Aasi, BP Abbott, Richard Abbott, Thomas Abbott, MR Abernathy, Kendall Ackley, Carl Adams, Thomas Adams, Paolo Addesso, RX Adhikari, et al. Advanced ligo. *Classical and quantum gravity*, 32(7):074001, 2015.

[5] F Acernese, M Agathos, K Agatsuma, D Aisa, N Allemandou, A Allocca, J Amarni, P Astone, G Balestri, G Ballardin, et al. Advanced virgo: a second-generation interferometric gravitational wave detector. *Classical and Quantum Gravity*, 32(2):024001, 2014.

[6] Yoichi Aso, Yuta Michimura, Kentaro Somiya, Masaki Ando, Osamu Miyakawa, Takanori Sekiguchi, Daisuke Tatsumi, and Hiroaki Yamamoto. Interferometer design of the kagra gravitational wave detector. *Phys. Rev. D*, 88:043007, Aug 2013.

[7] LIGO. Ligo: Facts.

[8] Carlton M Caves. Quantum-mechanical radiation-pressure fluctuations in an interferometer. *Physical Review Letters*, 45(2):75, 1980.

[9] Carlton M Caves. Quantum-mechanical noise in an interferometer. *Physical Review D*, 23(8):1693, 1981.

[10] M Tse, Haocun Yu, N Kijbunchoo, A Fernandez-Galiana, P Dupej, L Barsotti, CD Blair, DD Brown, SE Dwyer, A Effler, et al. Quantum-enhanced advanced ligo detectors in the era of gravitational-wave astronomy. *Physical Review Letters*, 123(23):231107, 2019.

[11] Haocun Yu, L McCuller, M Tse, L Barsotti, N Mavalvala, J Betzwieser, CD Blair, SE Dwyer, A Effler, M Evans, et al. Quantum correlations between the light and kilogram-mass mirrors of ligo. *arXiv preprint arXiv:2002.01519*, 2020.

[12] L McCuller, C Whittle, D Ganapathy, K Komori, M Tse, A Fernandez-Galiana, L Barsotti, P Fritschel, M MacInnis, F Matichard, et al. Frequency-dependent squeezing for advanced ligo. *Physical Review Letters*, 124(17):171102, 2020.

[13] Yuhang Zhao, Naoki Aritomi, Eleonora Capocasa, Matteo Leonardi, Marc Eisenmann, Yuefan Guo, Eleonora Polini, Akihiro Tomura, Koji Arai, Yoichi Aso, et al. Frequency-dependent squeezed vacuum source for broadband quantum noise reduction in advanced gravitational-wave detectors. *Physical Review Letters*, 124(17):171101, 2020.

[14] Stefan L Danilishin and Farid Ya Khalili. Quantum measurement theory in gravitational-wave detectors. *Living Reviews in Relativity*, 15(1):5, 2012.

[15] Aashish A Clerk, Michel H Devoret, Steven M Girvin, Florian Marquardt, and Robert J Schoelkopf. Introduction to quantum noise, measurement, and amplification. *Reviews of Modern Physics*, 82(2):1155, 2010.

[16] M. D. Lukin. *Modern Atomic and Optical Physics II, lecture notes*. 2005.

[17] Emil Zeuthen, Albert Schliesser, Jacob M Taylor, and Anders S Sørensen. Electrooptomechanical equivalent circuits for quantum transduction. *Physical Review Applied*, 10(4):044036, 2018.

[18] Emil Zeuthen, Eugene S Polzik, and Farid Ya Khalili. Gravitational wave detection beyond the standard quantum limit using a negative-mass spin system and virtual rigidity. *Physical Review D*, 100(6):062004, 2019.